A SORTING APPROACH TO THE MAGNETIC RANDOM ERRORS

M. Giovannozzi, R. Grassi, W. Scandale and E. Todesco *

Abstract

The problem of defining effective sorting strategies for the random errors of a magnetic lattice is analyzed. The final goal is to define a way of sorting the magnets in order to maximize the dynamic aperture. The proposed method is made up of three steps. Firstly, one defines quality factors based on the perturbative tools of nonlinear maps and normal forms. Secondly, the best quality factor for the model considered is chosen through tracking analysis. Thirdly, among some permutations of the magnets one chooses that one whose quality factor is better. The effectiveness a posteriori of the sorting strategy is checked through tracking. An application to sort the sextupolar errors of a lattice made only of LHC-like cells is given.

Submitted to Phys. Rev. E

Geneva, Switzerland

March 20, 1995

---

* INFN, Sezione di Bologna, Via Irnerio 46, I-40126 Bologna.

1 INTRODUCTION

One of the main issues in the construction of large hadron colliders like the CERN LHC [1] is the effect of the nonlinearities due to the unavoidable multipolar errors in the superconducting magnets. These sources of nonlinearities can be split into two parts: a systematic one, which is the same for all the magnets, and a random one, which depends on the magnet. The multipolar errors considerably reduce the stability domain around the closed orbit where one can safely operate with the beam.

In order to correct the effect of the random multipoles, one can consider the sorting approach, i.e. the definition of a rule for ordering the magnets according to the value of their random errors so that the stability domain is maximized [2]. The main problem is that, even for a small set of magnets, the number of the allowed permutations is huge: therefore quality factors (QF) based on analytical or numerical tools seem to be more appropriate than a direct computation of the dynamic aperture to evaluate the ordering rules [3]. A completely different approach is based on the definition a priori of intuitive sorting rules based on local compensation or symmetry considerations, and the evaluation of their effectiveness through tracking; these methods have been used for the analysis of the LHC lattice [4], [5], [6].

In this paper we propose a sorting strategy based on a mixed approach, where both analytical and numerical methods are used in order to devise the best ordering rule. The analytical tools are given by the discrete formalism of nonlinear transfer maps and perturbative theory for symplectic mappings (normal forms [7]), rather than with classical perturbative theory for flows, in order to be able to compute automatically the series up to high orders [8].

We have defined three quality factors: the norm of the nonlinear part of the map, the norm of the amplitude-dependent tuneshift, computed through non-resonant normal forms, and the resonance strength evaluated through resonant normal forms. All these quality factors have been used in literature for the analysis of the nonlinearities: the norm of the map [9] in order to evaluate the effect of the multipolar errors for different magnetic lattices; the tuneshift minimization [10] to compute the best values of the gradients of the corrector elements used to compensate the systematic errors in the LHC; the resonance strength minimization [3] to propose a sorting strategy for the HERA.

We believe that the selection of the best quality factor is strongly dependent on the model, and therefore it cannot be made a priori: for this reason, we numerically evaluated through tracking which QF shows the best correlation with the dynamic aperture for the considered model. Then, for a given number of permutations of the magnets, we selected the best ordering according to the QF. Permutations can be chosen either randomly or using some intuitive criteria based on local compensation or symmetry rules. Finally, the effectiveness of the ordering is checked through tracking. The ordering strategy is performed

2

over an high number of different realizations of the random errors: 100 seeds are considered for testing each rule to have a sufficient statistics. Our approach is not restricted to treat only one type of errors (for instance, only sextupoles), but can be applied to sort all the nonlinear contributions to the random errors at the same time.

In order to test the method, we considered a simplified cell lattice with only sextupolar errors; the results show a big gain in the short term dynamic aperture, which is consistent with the literature. The obtained gain is very good also compared to other known methods [4] [5]. The approach outlined in this paper is a promising first step towards the verification of the effectiveness of a sorting strategy for the LHC.

The plan of the report is the following: in section 2 we review the formalism of nonlinear maps of magnetic lattices and the theory of normal forms. In section 3 we define the quality factors which will be used to sort the magnets. The sorting strategy is described in section 4; the results relative to an LHC cell lattice are given in section 5, where also an accurate analysis of the global dynamics of one of the analyzed seeds is given.

2   NONLINEAR MAPS AND NORMAL FORMS

In this section we recall some definitions and notations which will be used in the followings. We consider the betatronic oscillations of a single particle in a circular accelerator; we denote by $\hat{\mathbf{x}} = (\hat{\mathbf{x}}, \hat{\mathbf{p}}_{\mathbf{x}}, \hat{\mathbf{y}}, \hat{\mathbf{p}}_{\mathbf{y}})$ the Courant-Snyder coordinates and by $\mathbf{z} = (\mathbf{z_1}, \mathbf{z_1^*}, \mathbf{z_2}, \mathbf{z_2^*})$ the complex coordinates which diagonalize the linear part of the motion, where $z_1 = \hat{x} + i\hat{p}_x$, $z_2 = \hat{y} + i\hat{p}_y$, and the $*$ indicates the complex conjugation. The motion of a single particle is represented by the one-turn map $\mathbf{F}$, which propagates the position $\mathbf{z}$ of a particle at a given section of the machine to the position $\mathbf{z}'$ at the same section after one turn [7]:

$$
\begin{aligned}
z_1' = F_1(\mathbf{z}) &= e^{i\omega_1}z_1 + \sum_{n \geq 2} \sum_{j_1+j_2+j_3+j_4=n} F_{1;j_1,j_2,j_3,j_4}\, z_1^{j_1} z_1^{*j_2} z_2^{j_3} z_2^{*j_4} \\
z_2' = F_2(\mathbf{z}) &= e^{i\omega_2}z_2 + \sum_{n \geq 2} \sum_{j_1+j_2+j_3+j_4=n} F_{2;j_1,j_2,j_3,j_4}\, z_1^{j_1} z_1^{*j_2} z_2^{j_3} z_2^{*j_4}.
\end{aligned}
\tag{1}
$$

Here ω_1 and ω_2 are the linear tunes, and $F_{i;j_1,j_2,j_3,j_4}$ are complex coefficients.

Using the perturbative approach [7] [11] [12] [13], one conjugates the one-turn map $\mathbf{F}$ to its normal form $\mathbf{U}$, which is invariant under a symmetry transformation, and can be written as the Lie series of an interpolating Hamiltonian h. We will express h in polar coordinates $\theta_1, \theta_2, \rho_1, \rho_2$, where θ are the phases and ρ are the amplitudes in the space of the normal coordinates where h is defined [13]. According to the symmetry transformation, one can define different types of normal forms which provide asymptotic series [14] for some nonlinear indicators of motion: the dependence of the frequency on the amplitude (nonresonant case),

3

the geometrical and dynamical parameters of the resonances (single resonance), and the position and the stability of the fixed points (double resonance). We restrict ourselves to sketching the first two types of normal forms, which will be used in the definition of the quality factors. A more detailed description of the normal form theory is given in Refs. [7] and [13].

<u>Nonresonant case</u>: the normal form is an amplitude-dependent rotation, and the interpolating Hamiltonian is a function of the amplitudes ρ_1, ρ_2

$$h(\rho_1, \rho_2) = \omega_1 \rho_1 + \omega_2 \rho_2 + \sum_{k_1+k_2 \geq 2} h_{k_1,k_2}\ \rho_1^{k_1} \rho_2^{k_2}, \tag{2}$$

which are also the nonlinear invariants. The derivatives of h with respect to ρ_1 and ρ_2 provide an analytical expression of the tune in its dependence on the amplitude [10].

<u>Single resonance</u>: if the linear tunes are close to a single resonance $[q, p]$, i.e. one has

$$q\omega_1 + p\omega_2 = 2\pi l + \epsilon \qquad\qquad q \in \mathbf{N} \qquad \mathbf{p}, \mathbf{l} \in \mathbf{Z} \tag{3}$$

with $\epsilon \ll 1$, it is useful to build a single-resonance normal form which retains in the Hamiltonian h both the detuning terms, such as in the previous case, and the terms relative to the resonance [13]. In this case the Hamiltonian has the property of being well-defined also for $\epsilon = 0$ (exact resonance), and of keeping the topology of the resonance. The Hamiltonian has a more complicated polynomial structure: it depends on the amplitudes ρ_1, ρ_2 and on one linear combination of angles $q\theta_1 + p\theta_2$

$$h(\theta_1, \theta_2, \rho_1, \rho_2) = \sum_{k_1,k_2 \geq 0}\ \sum_{l \geq 0} h_{k_1,k_2,l}\ (\rho_1)^{k_1+lq/2}(\rho_2)^{k_2+lp/2} \cos(l(q\theta_1 + p\theta_2) + \varphi_{k_1,k_2,l}). \tag{4}$$

The nonlinear invariants are h and $p\rho_1 - q\rho_2$. One can distinguish between the coefficients $h_{k_1,k_2,0}$, which produce amplitude-dependent tuneshift, and the other terms $h_{k_1,k_2,l}$ with $l \geq 1$, which do excite the resonance.

3   DEFINITION OF QUALITY FACTORS

In this section we define some indicators of nonlinearity, of increasing complexity, based on the analytical tools of one-turn maps and normal forms; these indicators will be used in the next sections as quality factors (QF) for the analysis of the random errors.

3.1 Q_1: Norm of the map

The simplest indicator of nonlinearity one can define is the norm of the nonlinear part of the map: in this case the QF does not take into account compensation

effects between different terms and different orders which, in principle, can be very relevant. A possible definition of the norm of the nonlinear part of the map is

$$Q_1(A, N) = \sum_{n=2}^{N} A^n \sum_{j_1+j_2+j_3+j_4=n} \sum_{i=1,2} |F_{i;j_1,j_2,j_3,j_4}|, \qquad (5)$$

where the coefficients $F_{i;j_1,j_2,j_3,j_4}$ have been defined in Eq. 1. It must be pointed out that since the one-turn map in a generic case is composed by different orders, one has to introduce an amplitude A to weight the various contributions: low values of A lead to a smaller contribution from the high orders, and viceversa. Since one is mainly interested in the behaviour close to the dynamic aperture, we suggest to fix A to the estimated value of the dynamic aperture.

The use of the norm of the map as quality factor was suggested us by some previous works [9], where this indicator was successfully used to make both a qualitative and a quantitative comparison of the dynamics of two large machines such as the HERA and the LHC.

3.2 Q_2: Norm of the tuneshift

A more complex indicator of nonlinearity is the tuneshift, i.e. the part of the tune which depends on the amplitudes. We have shown in the previous section that nonresonant normal forms provide perturbative series for the tuneshifts. Using these expressions, one can build a QF: let us define the sum of the squares of the tuneshifts as

$$t_{2M}(\rho_1, \rho_2) \equiv \frac{1}{2} \left[\left(\sum_{i=1}^{M} [\nu_x(\rho_1, \rho_2)]_i \right)^2 + \left(\sum_{i=1}^{M} [\nu_y(\rho_1, \rho_2)]_i \right)^2 \right], \qquad (6)$$

where $[.]_i$ denote homogeneous polynomials of order i, which are given by the derivatives of the Hamiltonian:

$$[\nu_x(\rho_1, \rho_2)]_i = \frac{\partial}{\partial \rho_1} [h(\rho_1, \rho_2)]_{i+1}$$

$$[\nu_y(\rho_1, \rho_2)]_i = \frac{\partial}{\partial \rho_2} [h(\rho_1, \rho_2)]_{i+1}; \qquad (7)$$

then, we define the quality factor Q_2 as sum of the squares of the tuneshifts averaged over the sum of the square of the invariants $\rho_1^2 + \rho_2^2 = A^2$:

$$Q_2(A; M) \equiv \sqrt{\frac{2}{\pi} \int_0^{\pi/2} t_{2M}(A \cos \phi, A \sin \phi) \, d\phi}. \qquad (8)$$

Q_2 is the average tuneshift at the amplitude A; it depends on the truncation order M. It is easy to verify that, starting from a map truncated at order N,

one can build a nonresonant normal form at most of order N, which provides a perturbative series for the tuneshift truncated at order $M = (N-1)/2$.

The correlation between dynamic aperture and tuneshift is a well-known feature of the effect of the systematic multipolar errors in the LHC. A correction scheme of the multipolar errors based on an analytical minimization of the tuneshift was found to be very effective [10], [15]. Indeed, it is well known (see for instance Ref. [7], chapter 6) that a complete correction of the tuneshift is not desirable, since no detuning makes all the resonances unstable.

3.3 Q_3: Norm of the resonances

We have shown in the previous section that the theory of normal forms allows one to conjugate the one-turn map to the Lie series of an Hamiltonian which retains the terms relative to the tuneshift and to a single resonance (see Eq. 4). Therefore, one can build a QF that is related to the strength of a single resonance $[p, q]$ by taking the norm of the resonant part of the interpolating Hamiltonian:

$$Q_3([p,q], A; L) = \sum_{l \geq 1} \sum_{2k_1 + 2k_2 + l(p+q) \leq L} |h_{k_1, k_2, l}| A^{2k_1 + 2k_2 + l(p+q)}, \qquad (9)$$

where also in this case A is an amplitude which has the same physical meaning as in the definition of Q_1 and Q_2, and L is the truncation order of the Hamiltonian which must satisfy $L \geq (p+q)$ to have nonzero contributions. If the normal form $\mathbf{U}$ is truncated at order N, its interpolating Hamiltonian has a truncation order of $L = N + 1$.

The definition of this quality factor was suggested by Ref. [3], where the strengths of single-resonances, computed through classical perturbative theory for hamiltonian flows at second order in the gradients, were used as QF in order to propose a sorting procedure for the magnets of HERA.

4 THE SORTING METHOD

We now describe the sorting procedure which will be applied to a model of LHC in the next section; the method is based on four steps.

- <u>Definition of quality factors.</u> Different quality factors are defined, that can be computed in a very short CPU time, even for a complex lattice.

- <u>Evaluation of the best quality factor.</u> The short-term dynamic aperture is evaluated and correlated with the QF. Note that from a theoretical point of view, there is no indication of the best QF. Therefore, the choice of the optimal QF can be made only numerically, i.e. analyzing a high number of random machines with different seeds, computing their dynamic aperture and their quality factors, and selecting the QF with the best correlation.

- Evaluation of the best ordering. Having selected the QF, one has a fast
  method to distinguish between good and bad sequences of magnets; there-
  fore, for each seed which generates a sequence of random errors, one can
  consider a large set of permutations of the magnets, and check for each
  permutation the effect on the QF. Clearly, if the number of the random
  magnets which have to be ordered is greater than 10, it is possible to check
  only a small subset among all the existing permutations: indeed, one can
  either choose permutations randomly, or using some intuitive criteria based
  for instance on local compensation or on the symmetries of the lattice.

- Tracking check. When the best sequence of magnets is selected using the
  above-described procedure, one has to check its effectiveness through track-
  ing. In order to have results that are statistically significant, this test has
  to be repeated for many different seeds.

5 APPLICATIONS TO AN LHC CELL LATTICE

5.1 The model

We have considered a simplified LHC cell lattice; each cell has 6 dipoles and a
phase advance of 90°. Previous studies [4], [6] have shown that local compensation
and symmetry rules become very effective over a sequence of cells which covers
two periods of betatronic oscillations. Therefore, we analysed a lattice made up
of 8 cells of the LHC, plus a phase shifter in order to set the linear tunes of the
model to $\nu_x = 2.28$ and $\nu_y = 2.31$ without changing the phase advance of the cell.
Since we are analyzing only a fraction of the machine, the absolute values of the
dynamic aperture cannot be directly compared to the full lattice results: only the
relative values (i.e. the gain obtained by the sorting procedure) are significant.

We considered a model with only sextupolar errors, which is very sensitive
to a sorting strategy. It is customary to define the normal sextupolar integrated
gradient as

$$K_2 \equiv \ell \frac{1}{B_0 \rho_0} \frac{\partial^2 B_y}{\partial x^2}, \tag{10}$$

where ℓ is the length of the magnetic element, B_0 is the constant bending field
and ρ_0 is the radius of curvature. In our model the systematic part of K_2 (i.e. its
mean value) has been set to zero, since in the real machine it can be compensated
with the standard corrector magnets. The standard deviation of the random part
of K_2 has been fixed to

$$\sigma_{K_2} = 8.5872 \times 10^{-3} m^{-2}. \tag{11}$$

The distribution is assumed to be gaussian truncated at three σ_{K_2}.

5.2 QF correlation

We have computed the correlation between the dynamic aperture and the QF's for 100 seeds of random machines. The dynamic aperture was computed over 1000 turns; it is expressed in meters normalized at $\beta_{max} = 169m$.

In Fig. 1a we show the distribution in the dynamic aperture of the 100 random machines without ordering the magnets. One finds a wide distribution of the dynamic aperture according to the different seeds; this gives a first indication on the validity of a sorting strategy. The correlation with the QF based on the norm of the map Q_1, on the tuneshift Q_2, and on the strength of the resonance $[3,0]$ is given respectively in Figs. 1b, 1c and 1d. We have pointed out in the section 3 that in order to weight the different perturbative orders which contribute to the QFs (see Eqs. 5, 8, 9) one has to insert an average value of the dynamic aperture, which can be evaluated only through tracking; in our case we fixed this amplitude to the average of the distribution of the unsorted machines (i.e. 0.2 m). The norm of the map was evaluated up to order $N = 6$; the norm of the resonances was computed using the interpolating Hamiltonian truncated at order $L = 7$, and the tuneshift norm was evaluated using the first two tuneshift orders $M = 2$.

The analysis of the data shows that the norm of the map Q_1 has a poor correlation with the dynamic aperture. This result is not in contradiction with Ref. [9]: even though the norm of the different orders of the map can be useful to compare different machines, it proves to be not enough precise to select good and bad seeds of the same machine. The best QF for the considered model is the tuneshift norm Q_2; also resonance $[3,0]$, which is the first resonance excited by sextupoles, shows a rather good correlation. All the correlations with resonances up to order 7 were evaluated: two of them (e.g. resonance [2,-1] and [7,0]) are shown in Fig. 2. A theoretical explanation of these results seems very hard, and would need a very careful analysis of the interaction between the nonlinearities in the lattice and resonances, tuneshifts, and dynamic aperture. We believe that this is still an open problem: for this reason we have proposed to select the best QF using the correlation with the results of tracking simulations.

5.3 Sorting, tracking check, and comparison with local compensation

Using the results of the previous analysis, we have implemented two sorting strategies: the first one (SORT1) based on the tuneshift norm Q_2, and the second one (SORT2) on the strength of the resonance $[3,0]$. Moreover, we also implemented a rule based on the principle of local compensation (SORT0) which was defined through a very careful numerical analysis of the LHC cell lattice, as described in references [4] and [5]. We implemented SORT0 to cross check our method with the most effective sorting rule known for the same model.

Having fixed the number of the magnets to be sorted to 48, the number of

possible permutations is huge (approximately 10^{61}). Since a complete check of all the permutations is not feasible, we decided to rearrange the magnets according to two different rules: in the first case (labelled by SORT11 and SORT21) we simply made P random permutations, with P ranging from 1 to 500. In the second case (labelled by SORT12 and SORT22) we grouped the 48 dipoles in 24 pairs such that in each pair the sum of the sextupoles errors is minimized, producing a 'first-order local compensation'; then, we considered P random permutations of the 24 pairs, with P ranging from 1 to 500.

In Fig. 3a we show the distribution in the dynamic aperture for 100 different seeds of the LHC cell lattice ordered with the local compensation rule SORT0; in agreement with the literature [4], [6], one finds an impressive improvement in the dynamic aperture (about a factor 2.7). The results relative to the rule SORT11, with an increasing number of permutations, are also shown in Fig. 3 (Fig. 3b: $P = 20$, Fig. 3c: $P = 100$, Fig. 3d: $P = 500$). The gain in the dynamic aperture is significant, even if it is worse than SORT0 (about a factor 1.9 with respect to the unsorted model). If the number of permutations is increased, one obtains better machines, as expected. Indeed, there is a saturation effect in the dependence on P; we believe that this feature is due to the fact that the QF has a correlation pattern which is always better for bad machines than for good ones (see Figs. 1 and 2). This means that the QF easily recognizes bad machines, but it is not very efficient in selecting good machines: this could justify the saturation effect.

In Fig. 4 we show the distribution in the dynamic aperture for 100 different seeds of the model ordered with the rule SORT12, where the random permutations are carried out on pairs of approximately self-compensating errors. Also in these cases we show the dependence on the number of permutations (Fig. 4a: $P = 1$, Fig. 4b: $P = 20$, Fig. 4c: $P = 100$, Fig. 4d: $P = 500$). The sorting rule is more effective than SORT0 (the gain with respect to the unsorted machine in the average dynamic aperture is about a factor 3.1), especially if one considers the effect on bad machines, whose dynamic aperture is increased by a factor two. Also in this case there is a saturation effect in the dependence on P: it must be pointed out that even if the ordering with $P = 100$ has an average dynamic aperture which is slightly higher than the case $P = 500$, this last ordering is more effective since the rms of the distribution is 30% smaller. A simple pairing of the magnets without QF minimization provides a gain of a factor 1.4 (case SORT12, $P = 1$). In Fig. 5 we show the distribution of the dynamic aperture for the rule SORT22 (Fig. 5a: $P = 20$, Fig. 5b: $P = 100$); the gain in the dynamic aperture is significant, even if it is lower than the gain obtained with rule SORT12. From the above analysis it turns out that for the considered model the most effective strategy is the tuneshift minimization over pair permutations, which leads to very good gains in the average dynamic aperture.

5.4 Effect of the sorting procedure on global dynamics

Finally, a check of the effect of the sorting procedure was carried out through a very accurate analysis of the dynamics both in phase space and in frequency space, according to the numerical techniques of frequency analysis originally developed for celestial mechanics [16]. A stability diagram and its related tune footprint gives a description of the stability domain in phase space and in frequency space. This second diagram is very relevant since it provides the tune distribution, and therefore it allows one to understand which are the most dangerous resonances and their effect on the stability of motion.

In order to build these diagrams, we consider all the particles with the following initial conditions

$$
\begin{aligned}
\hat{x} &= r \cos \alpha & \hat{p}_x &= 0 \\
\hat{y} &= r \sin \alpha & \hat{p}_y &= 0
\end{aligned}
\tag{12}
$$

we make a fine scan over r and α (100 steps in each variable respectively), with $r \in [0, R]$ and $\alpha \in [0, \pi/2]$. For each initial condition we track over 1000 turns, and for the stable conditions we plot the corresponding point in the $(\hat{x}, \hat{y})$ diagram and the related nonlinear frequencies in the tune diagram computed as the average phase advance. For the sake of brevity, we only show two couples of these diagrams: one couple for a random machine with average dynamic aperture (Fig. 6a and Fig. 7), and another couple for the same machine after the sorting carried out using rule SORT12 (Fig. 6b and Fig. 8). The polar scanning in the initial conditions (see Eq. 12) is carried out with an external cycle over α, and an internal one over r: each time an orbit is lost before the considered number of iterates, r is taken as the first lost particle and the tracking is continued with the successive value of α. In this way, 'holes' in the dynamic aperture give rise to the spikes which can be observed in Fig. 6: in fact, this algorithm can lead to underestimate the stability domain, but has the advantage of avoiding the inclusion of islands unconnected to the stability boundary for the dynamic aperture evaluation.
The analysis of the Figs. 6, 7 and 8 leads to the following observations.

- The shape of the stability domain in the plane $(\hat{x}, \hat{y})$ is quite irregular, and it is radically modified by the sorting procedure (i.e. the ordering of the magnets does not simply rescales the stability boundary, but changes its shape, as expected).

- Tune footprint diagrams show that the ordering procedure not only minimizes the tuneshift, but also changes the low order tuneshift coefficients so that different zones of the frequency space are occupied by the random and sorted machine.

- In the case analyzed, the unsorted machine has very strong second order tuneshifts which lead to the folding of the tune footprint; conversely, the

sorted machine has tuneshifts which are dominated by the first order. Computations carried out over other seeds show that this feature depends on the seed.

- In the sorted machine the effect of resonances is stronger and more clearly visible: this happens because, having minimized the tuneshift, the islands become larger. Notwithstanding this effect, the stability domain of the sorted machine is three times bigger than the unsorted one. The island width is clearly shown in the tune footprint as an high density of initial conditions on resonance lines, and an empty region around them (see for instance resonances $[1, -4]$ and $[7, 0]$ in Fig. 8). On the other hand, some resonances seem to be not excited (i.e. resonances $[2, -5]$ and $[6, 1]$ in the same Figure): we checked that these resonances have zero or very low QF with no correlation with the dynamic aperture.

- Finally, one can observe that resonance $[3, 0]$ is very far from the tune footprint: nevertheless, this resonance shows the best correlation with the dynamic aperture. An explanation of this feature needs deeper investigations.

We conclude this section by pointing out the considerable amount of phenomenological information which is given by the stability diagram and the related tune footprint: we believe that this numerical tool should be better exploited in order to have a clearer picture of the dynamics. Unfortunately, the computation of such diagrams requires a large amount of CPU time. For this reason, the definition and the investigation of numerical tools which allow one to compute nonlinear frequencies with good accuracy and low number of turns would be highly desirable.

6   CONCLUSIONS

We have defined a sorting strategy which has the fundamental property of being very flexible: we believe that this feature is very important, since it seems clear from the numerous papers on the subject that sorting strategies are strongly dependent on the model. The proposed approach is based on a mixed technique which exploits both tracking simulations for determining the best quality factors, and analytical techniques to evaluate in a fast way the best permutations of the magnets. This technique can be integrated by other intuitive criteria used for determining the set of permutations, based on the symmetry of the lattice. We have successfully applied the outlined strategy to an LHC cell lattice, finding gains which are very good also compared to other known methods.

In order to check the effectiveness of the sorting strategy for the LHC, one should make a deeper investigation of more realistic lattices, where one has to take into account also the presence of various multipolar components, the necessity of having a compensation which is valid also for different settings of the machine,

and the limited precision of the measurements of the random components of the magnets. The approach outlined in this paper has proved to be a useful tool for the analysis of these problems.

7 ACKNOWLEDGEMENTS

References

[1] The LHC study group, CERN **91–03** (1991).

[2] R. L. Gluckstern and S. Ohnuma, IEEE Transactions on Nuclear Science **NS-32**, 2314-16 (1985).

[3] F. Willeke, DESY HERA **87–12** (1987).

[4] W. Scandale, L. Wang, CERN SPS (AMS) **89-22** (1989).

[5] W. Scandale, L. Wang, CERN SPS (AMS) **89-41** (1989).

[6] V. Ziemann, CERN SL (AP) **94–59** (1944).

[7] A. Bazzani, E. Todesco, G. Turchetti and G. Servizi, CERN **94–02** (1994).

[8] A. Bazzani, M. Giovannozzi and E. Todesco, *Comp. Phys. Comm.*, in press.

[9] R. Kleiss, F. Schmidt and F. Zimmermann, Part. Acc. **41**, 117–32 (1993).

[10] W. Scandale, F. Schmidt and E. Todesco, Part. Accel. **35**, 53–81 (1991).

[11] A. D. Brjuno, Math. USSR Sbornik **12**, 271–311 (1970).

[12] E. Forest, M. Berz and J. Irwin, Part. Accel. **24**, 91–113 (1989).

[13] E. Todesco, Phy. Rev. E **50**, R4298–301 (1994).

[14] G. Turchetti, in *Number theory and physics*, edited by J. M. Luck and P. Moussa (Springer Verlag, Berlin–Heidelberg, 1990) pp. 223–34.

[15] M. Giovannozzi, W. Scandale and F. Schmidt, CERN SL (AP) **93-29** (1993).

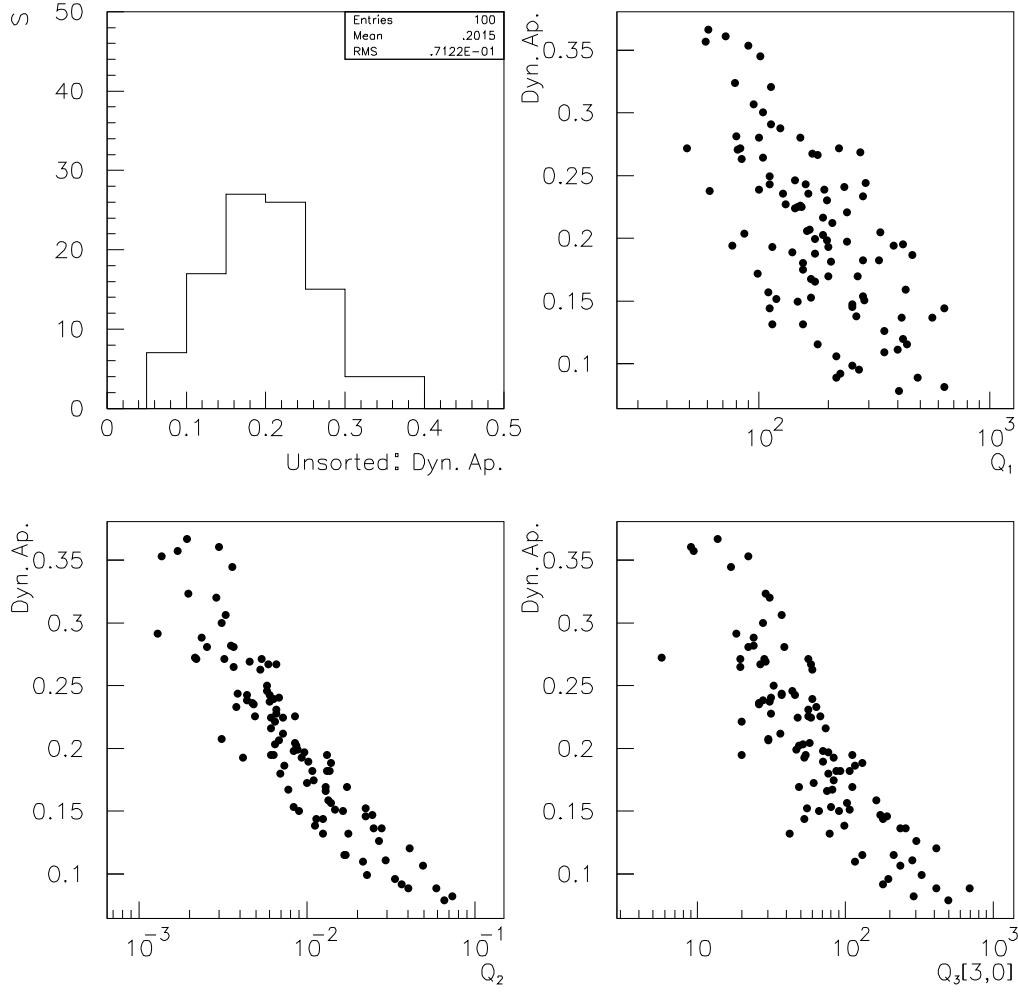[16] J. Laskar, Physica D **67**, 257–81 (1992).

Figure 1: Distribution of the dynamic apertures for the random machine, 100 seeds (a). Correlation of the quality factors Q_1 (b), Q_2 (c), $Q_3[3,0]$ (d) with the dynamic aperture for the random machine, 100 seeds.
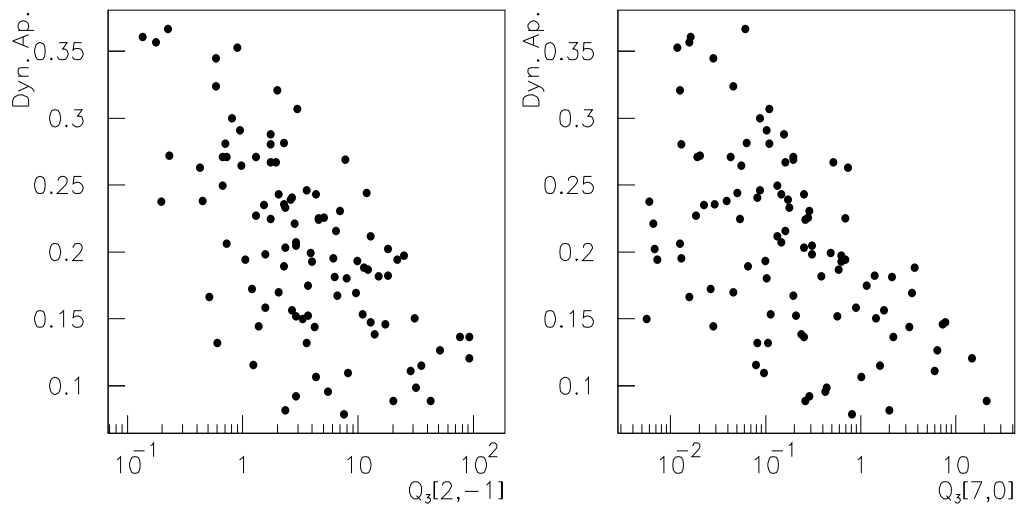
Figure 2: Correlation of the quality factors $Q_3[2, -1]$ (a), $Q_3[7, 0]$ (b), with the dynamic aperture for the random machine, 100 seeds.
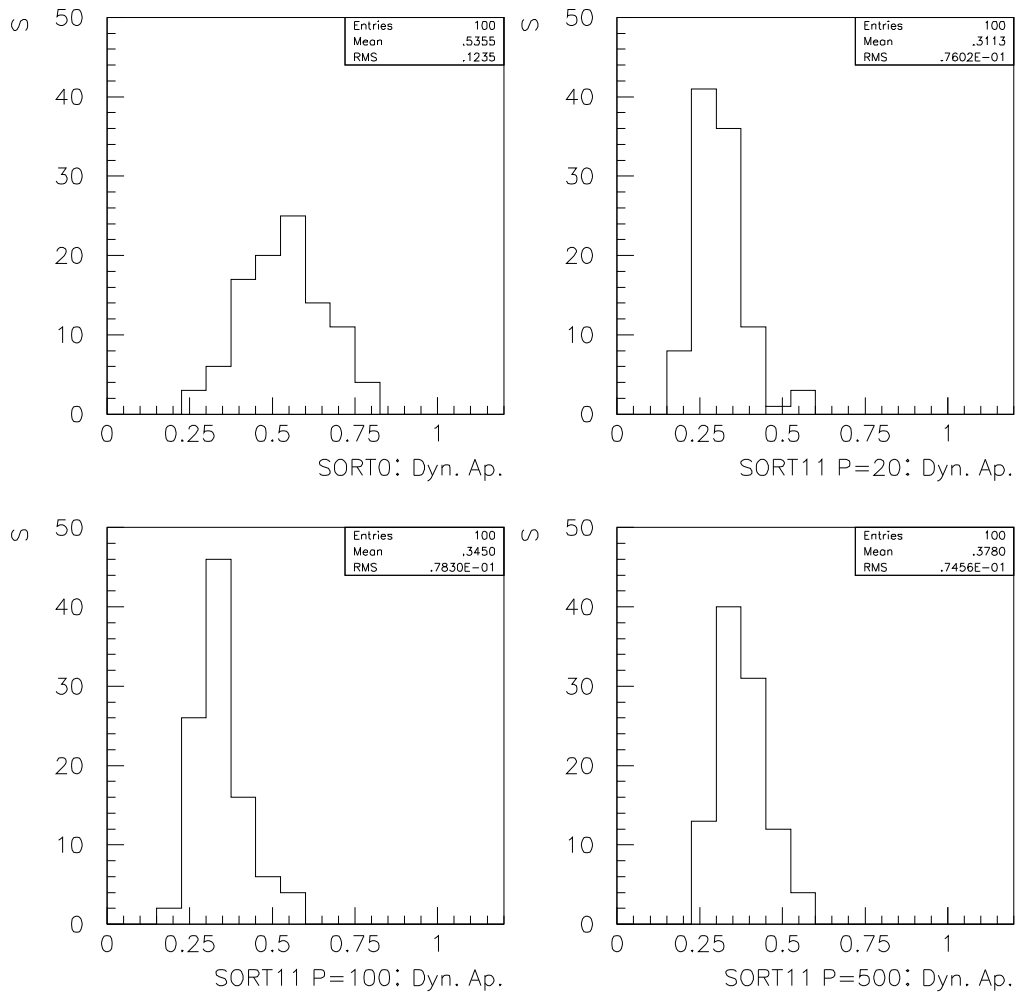
Figure 3: Distribution of the dynamic apertures for the SORT0 machine, 100 seeds (a). Distribution of the dynamic apertures for the SORT11 machine, 100 seeds $P = 20$ (b), $P = 100$ (c), $P = 500$ (d).
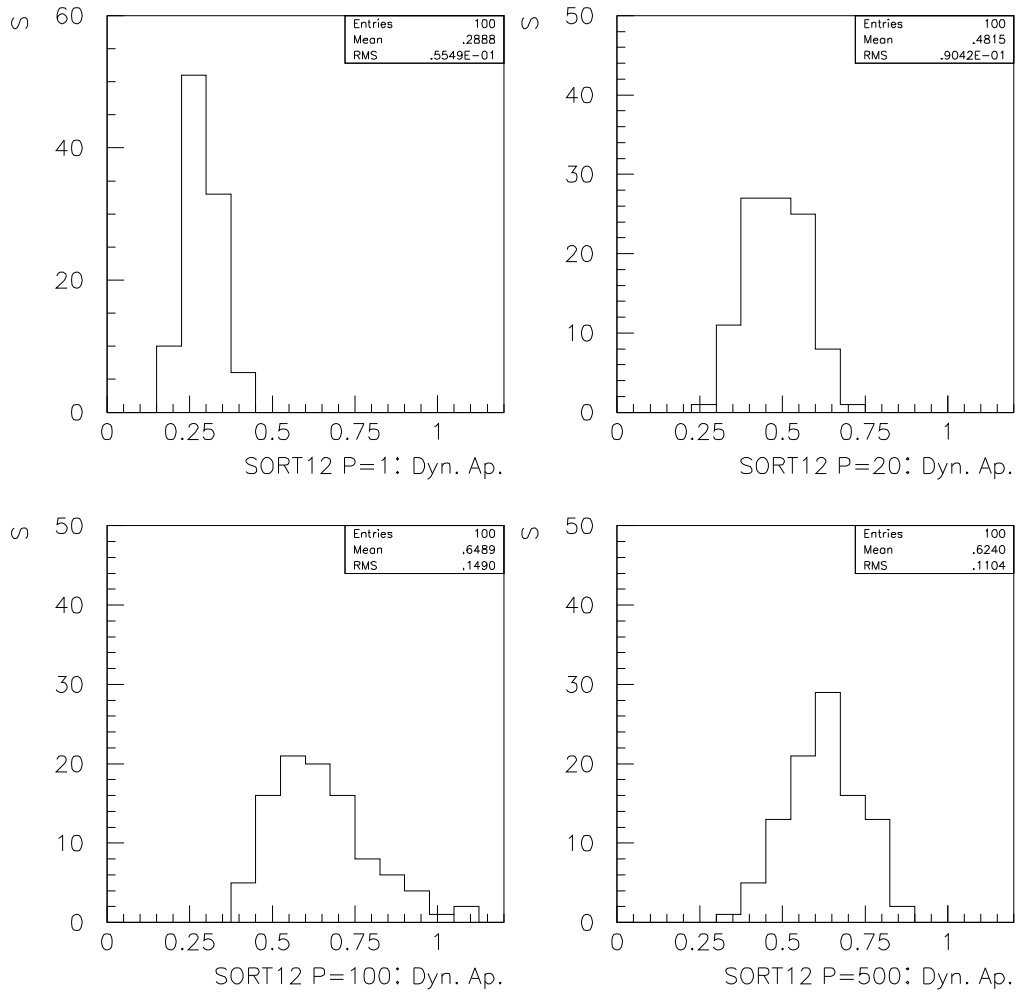
Figure 4: Distribution of the dynamic apertures for the SORT12 machine, 100 seeds $P = 1$ (a), $P = 20$ (b), $P = 100$ (c), $P = 500$ (d).
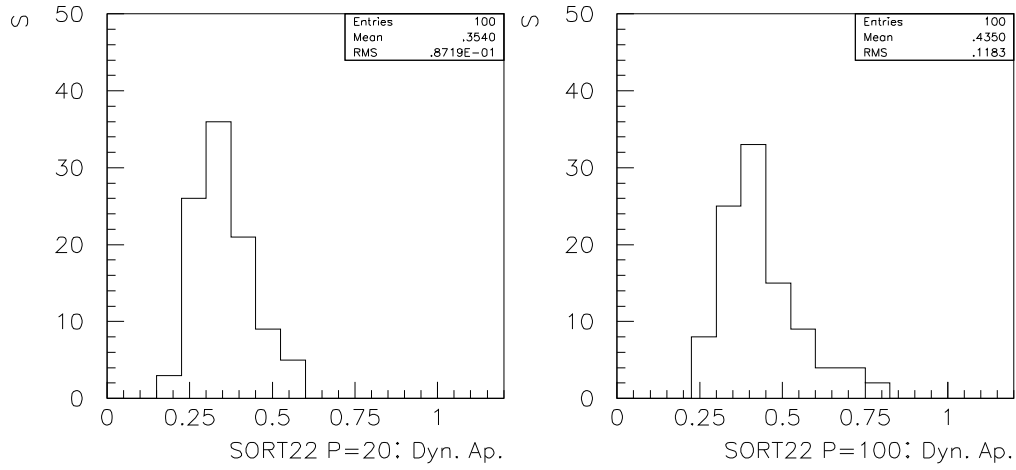
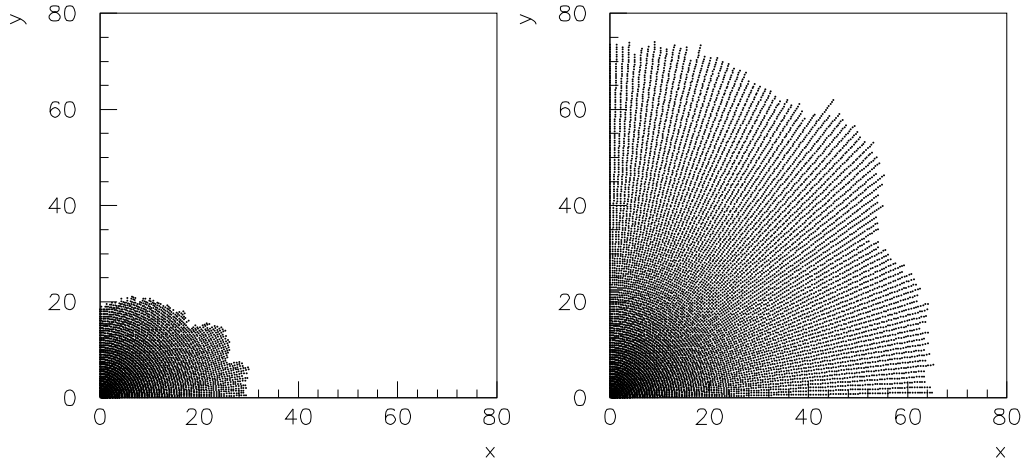Figure 5: Distribution of the dynamic apertures for the SORT22 machine, 100 seeds $P = 20$ (a), $P = 100$ (b).

Figure 6: Stability diagrams for one of the seeds with average unsorted dynamic aperture: before sorting (a) and after sorting with rule SORT12 (b).
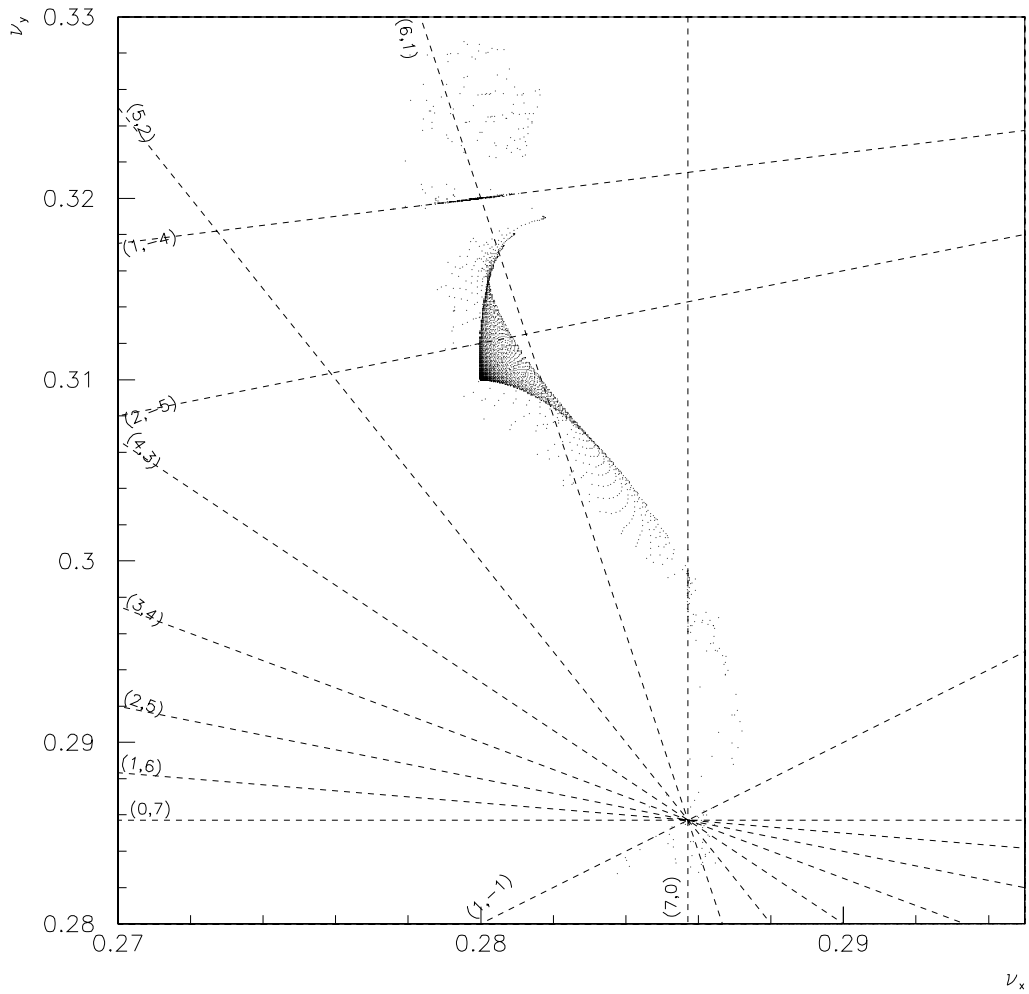
Figure 7: Tune footprint and resonance lines up to order 7 of the unsorted machine whose stability diagram is shown in Fig. 6a.
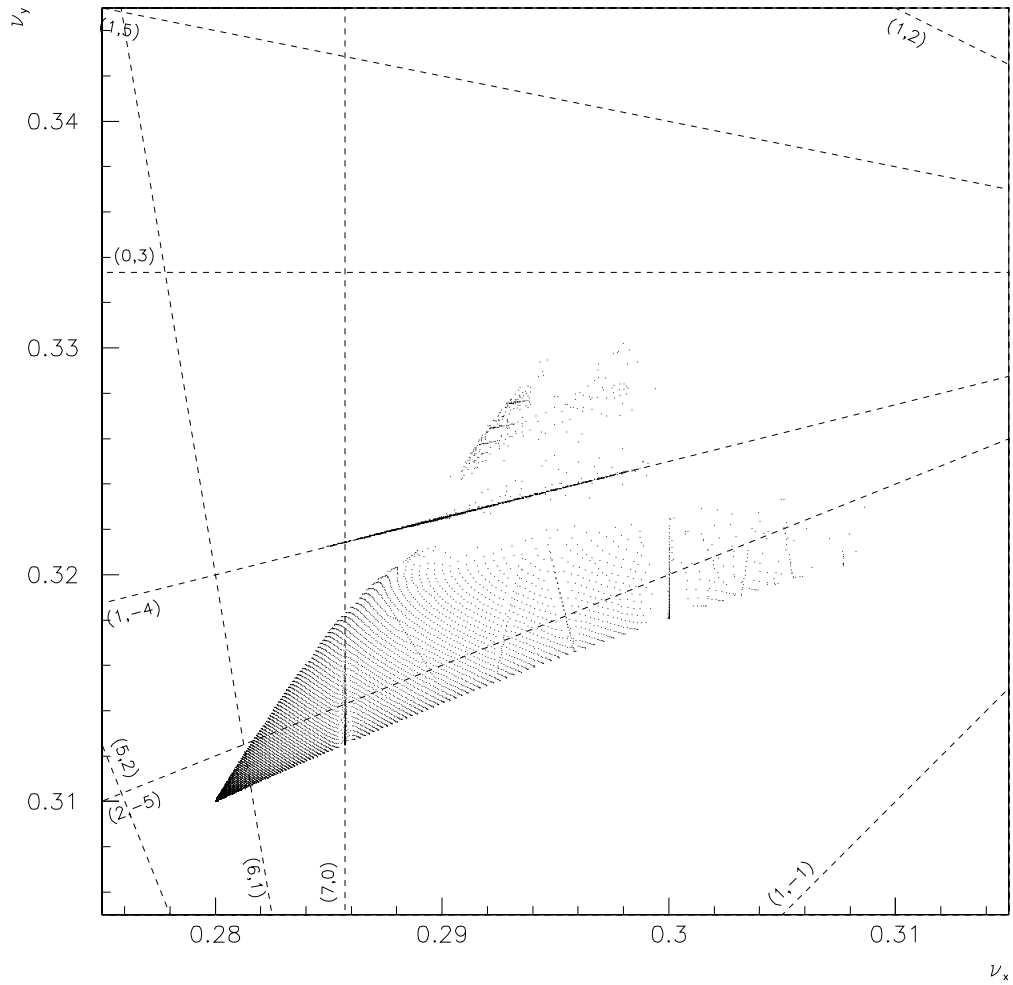
Figure 8: Tune footprint and resonance lines up to order 7 of the SORT21 machine whose stability diagram is shown in Fig. 6b.